Science Signaling
AAAS

stke.sciencemag.org/cgi/content/full/13/625/eaay8248/DC1

Supplementary Materials for

4-1BB costimulation promotes CAR T cell survival through noncanonical NF-κB signaling

Benjamin I. Philipson, Roddy S. O'Connor, Michael J. May, Carl H. June, Steven M. Albelda, Michael C. Milone*

*Corresponding author. Email: milone@pennmedicine.upenn.edu

Published 31 March 2020, *Sci. Signal.* **13**, eaay8248 (2020)
DOI: 10.1126/scisignal.aay8248

This PDF file includes:

Fig. S1

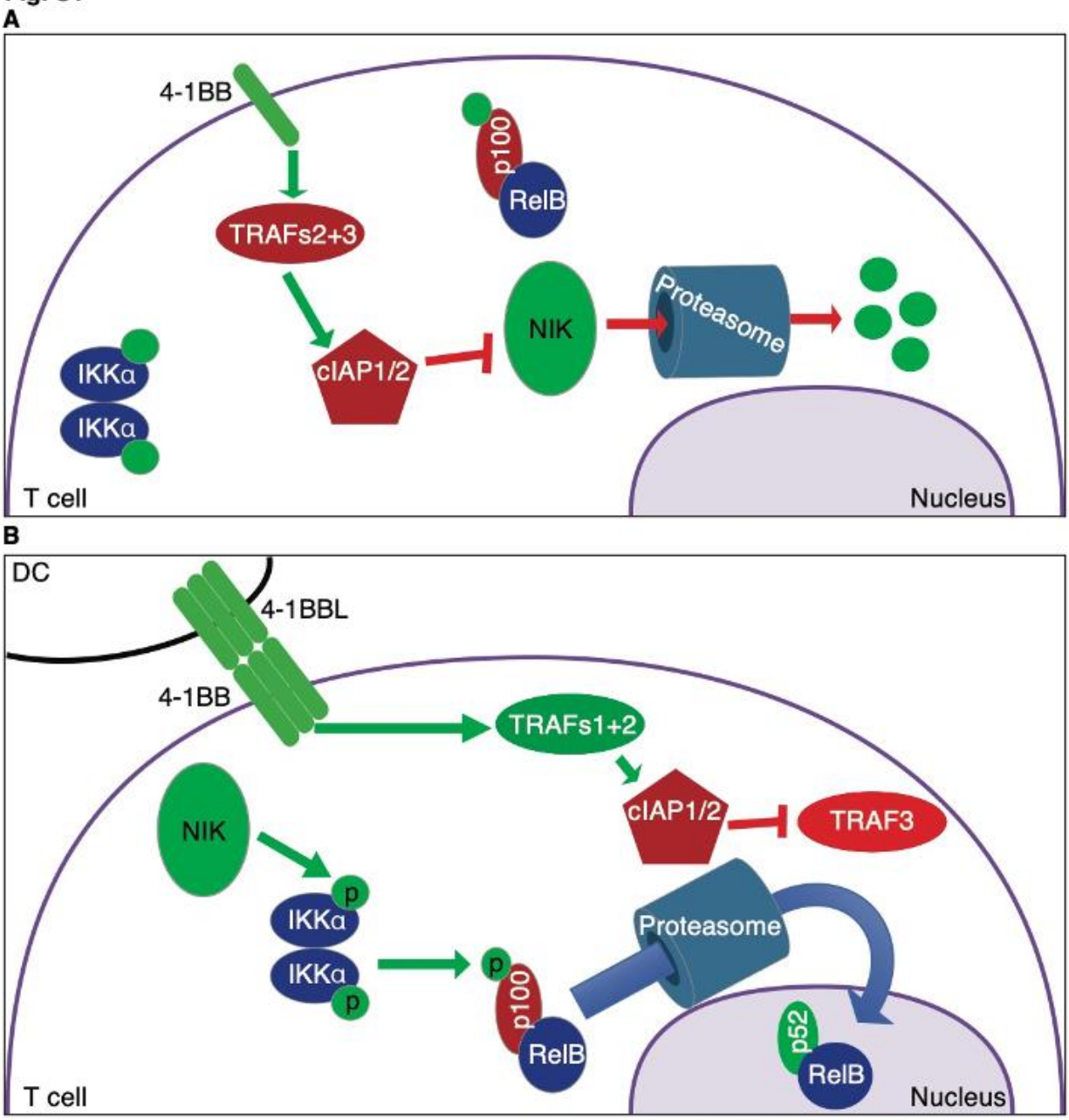

Fig. S1. The ncNF-κB pathway. (**A**) 4-1BB is expressed as a monomer or dimer before ligand binding. At baseline, 4-1BB associates with TRAF2 and TRAF3, which recruit the E3 ubiquitin ligases cIAP1 and cIAP2 to NIK. NIK is subsequently polyubiquitylated and degraded by the proteasome. (**B**) Upon ligand-induced trimerization of 4-1BB, TRAF1 is recruited to form a heterotrimer with TRAF2. Upon recruitment, TRAF1 and TRAF2 redirect cIAP1 and cIAP2 to TRAF3 and away from NIK, which enables NIK to accumulate in the cytosol. NIK binds to IKKα, p100, and RelB, generating a complex that leads to the phosphorylation of IKKα and p100. Upon phosphorylation, p100 is polyubiquitylated and partially degraded by the proteasome to generate p52. This partial degradation reveals a nuclear localization sequence, which enables translocation of the RelB-p52 heterodimer to the nucleus.

Fig. S2

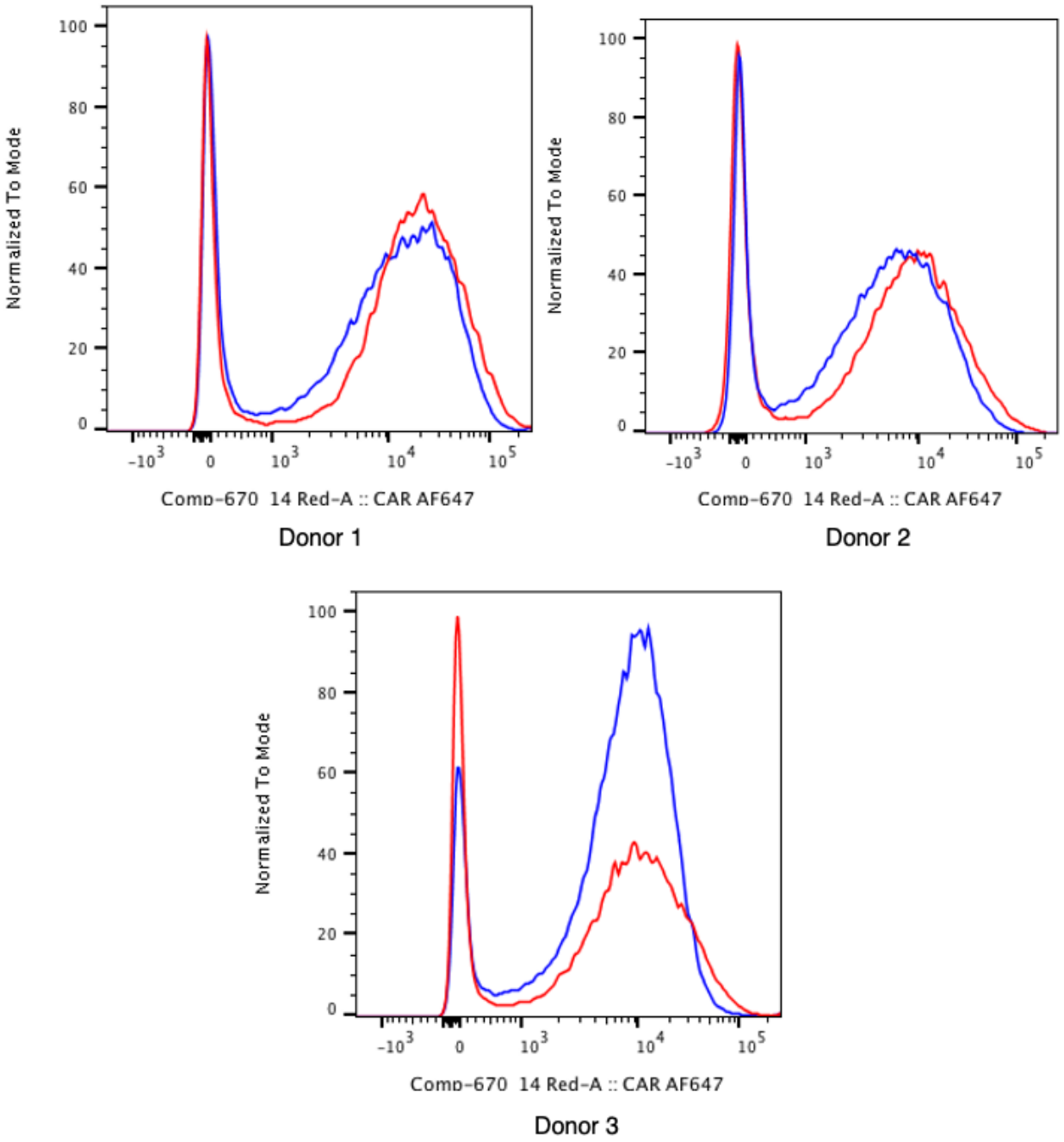

Fig. S2. CAR expression on T cells from three donors expanded by irradiated Nalm6 cells. 28ζ CAR T cells (red) and BBζ CAR T cells (blue) from three individual donors used in the experiments in Fig. 1A were analyzed by flow cytometry as described in Materials and Methods. Representative histograms are shown.

Fig. S3

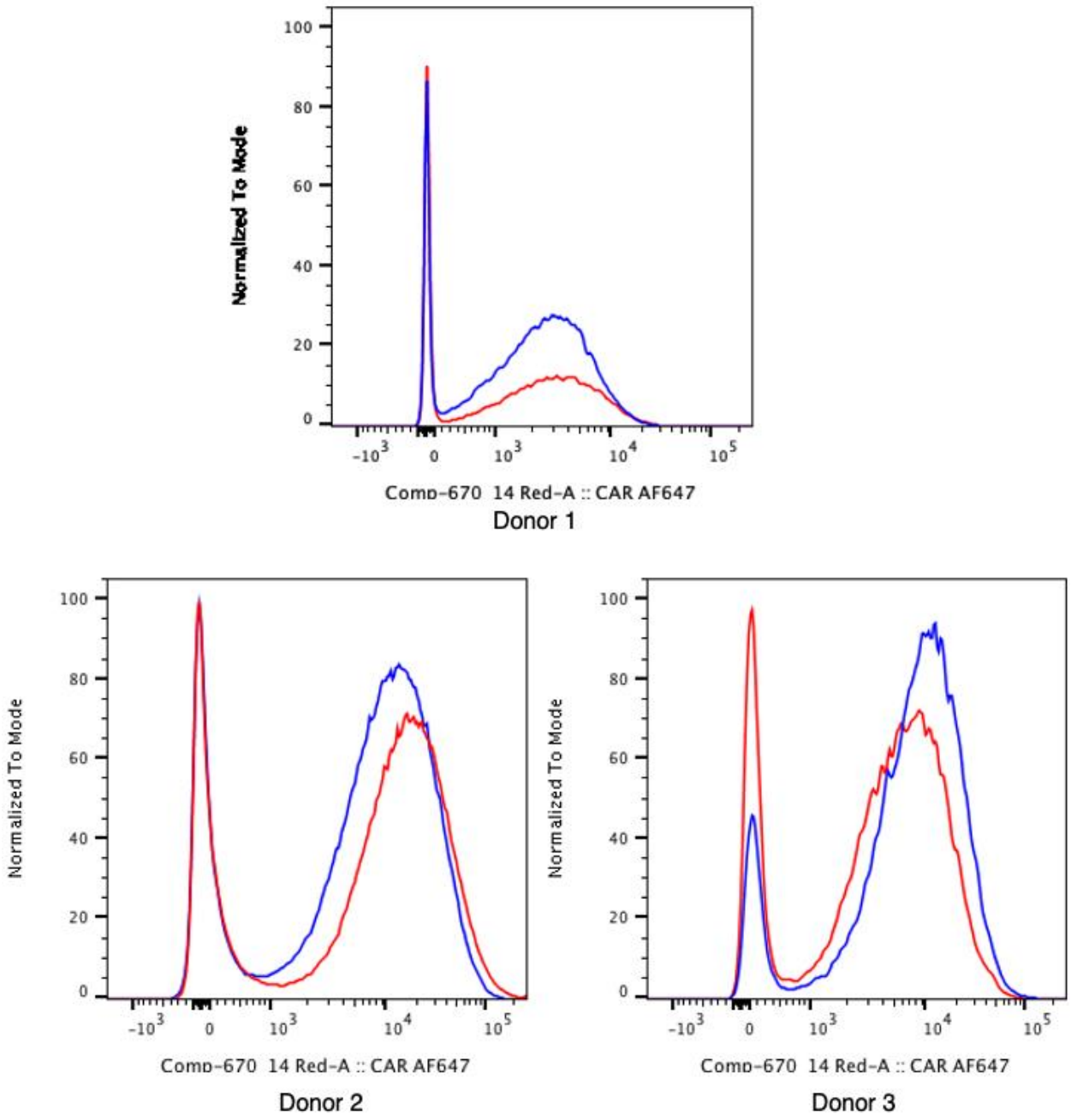

Fig. S3. CAR expression on T cells from three donors expanded by anti-CD19 beads. 28ζ CAR T cells (red) and BBζ CAR T cells (blue) from three individual donors used in the experiments shown in Fig. 1E were analyzed by flow cytometry. Representative histograms are shown.

Fig. S4

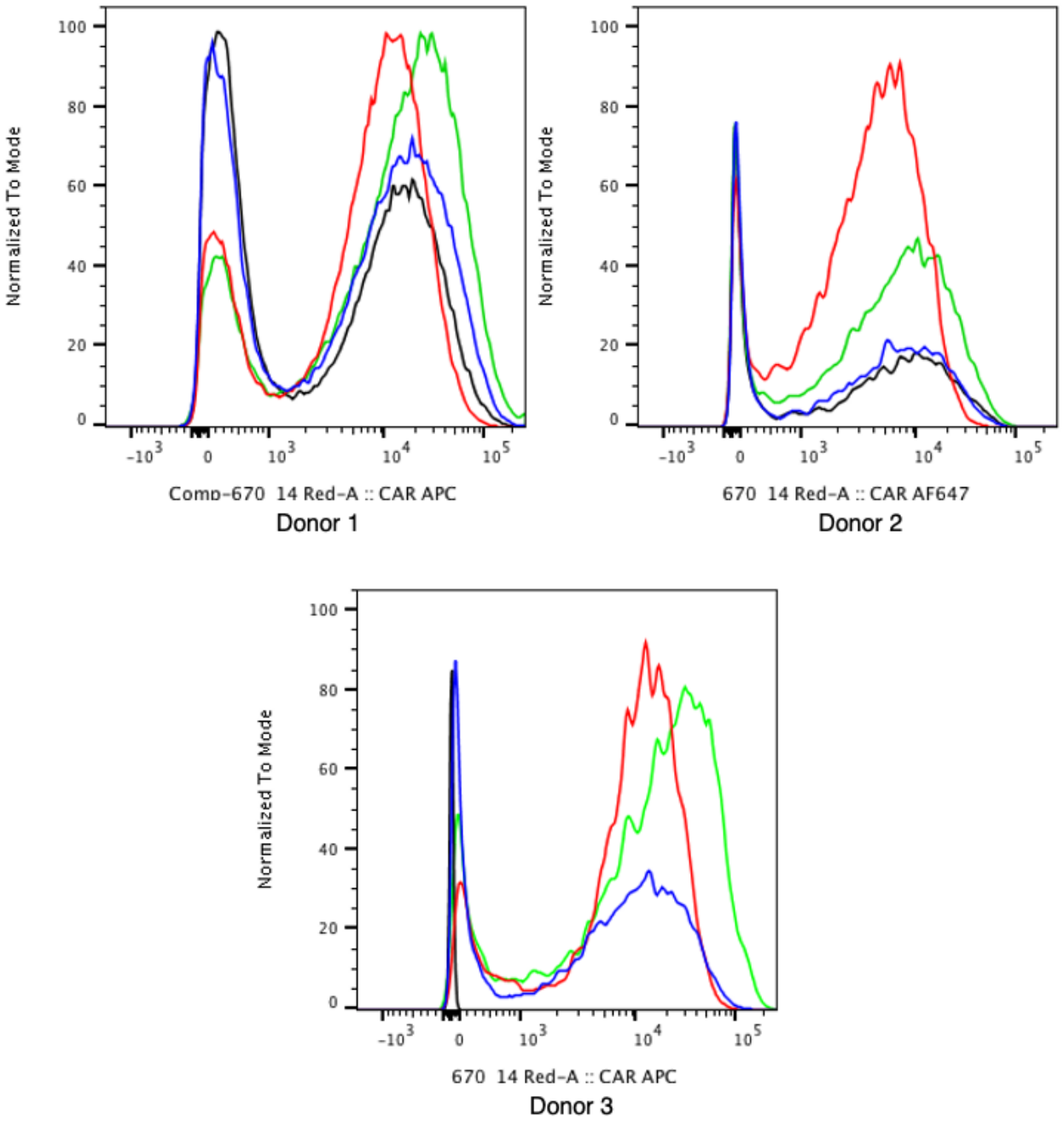

Fig. S4. CAR expression on T cells from three donors activated by anti-CD19 beads for signaling assays. Δζ (black), ζ (green), 28ζ (red), and BBζ (blue) CAR T cells from three individual donors used in the experiments shown in Figs. 2 and 4 were analyzed by flow cytometry. Representative histograms are shown.

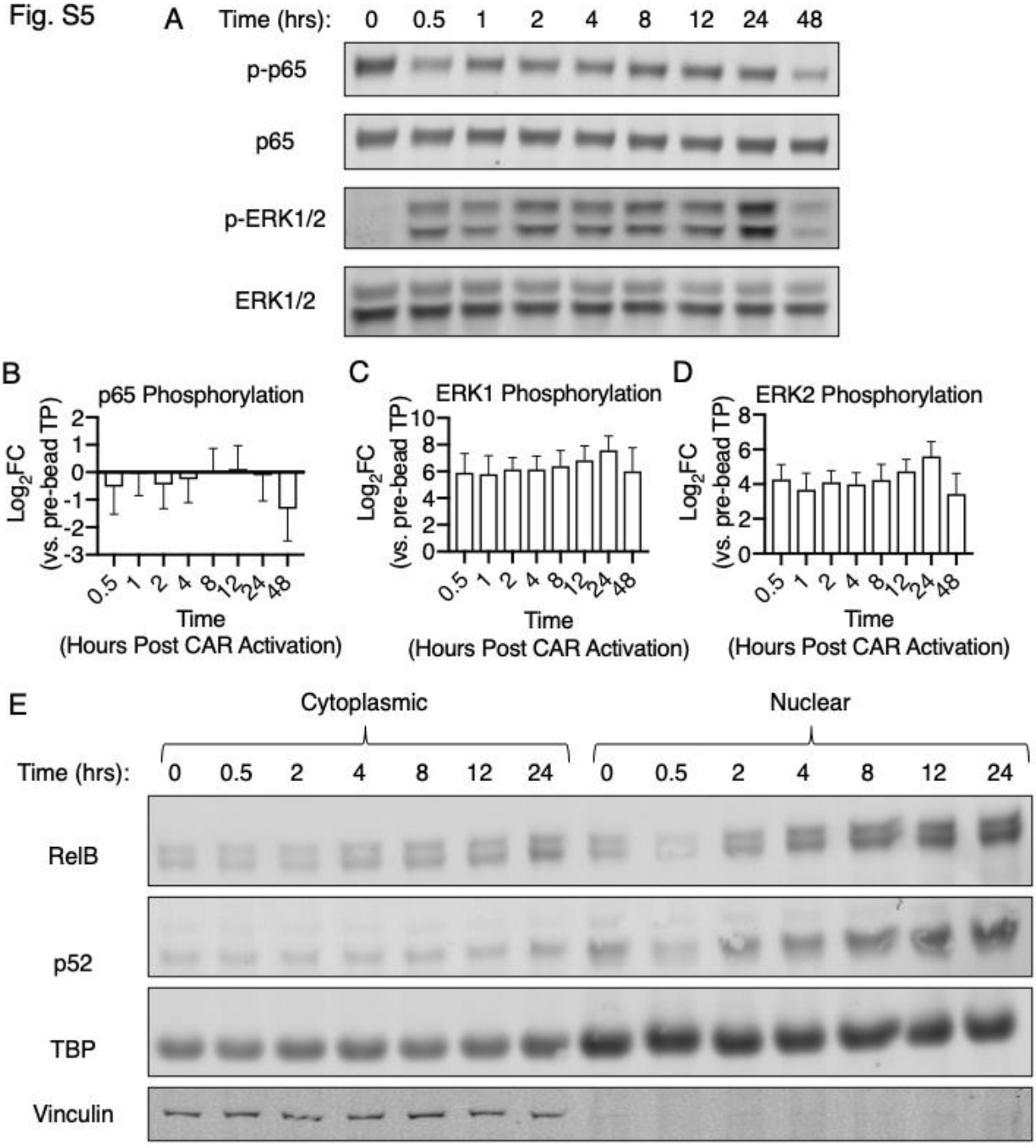

Fig. S5. Anti-CD19 BBζ CAR activation induces T cell signaling. (**A**) Representative Western blotting analysis of phosphorylated and total p65 and ERK1/2 proteins in BBζ CAR T cells incubated for the indicated times with stimulator beads. (**B** to **D**) Quantification of the relative amounts of phosphorylated p65 (B), phosphorylated ERK1 (C), and phosphorylated ERK2 (D) in the indicated samples from the experiments represented in (A). Data in (B) to (D) are from three donors in three independent experiments. (**E**) Western blotting analysis of RelB, p52, TBP, and vinculin in the cytoplasmic and nuclear fractions of BBζ CAR T cells incubated for the indicated times with stimulator beads. These T cells are from a second donor, the first of which is shown in Fig. 3E. Data are representative of two independent experiments.

Fig. S6

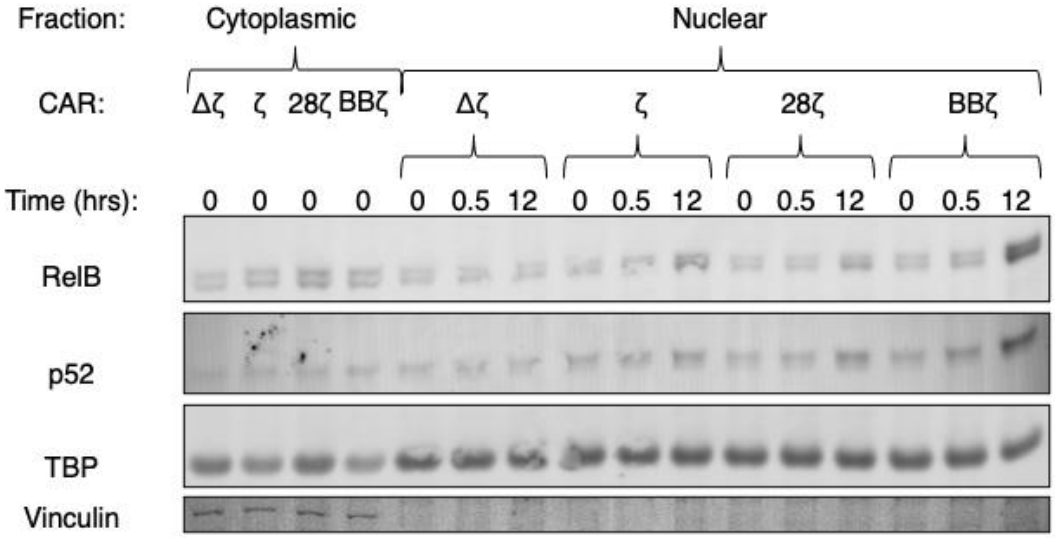

Fig. S6. Additional representative Western blotting analysis of nuclear and cytoplasmic fractions to compare anti-CD19 CAR signaling. Representative Western blotting analysis of RelB, p52, TBP, and vinculin in the cytoplasmic and nuclear fractions of the indicated CAR T cells at the indicated times after incubation with stimulator beads. Loss of vinculin indicates the nuclear fractions. These data complement those in Fig. 4.

Fig. S7

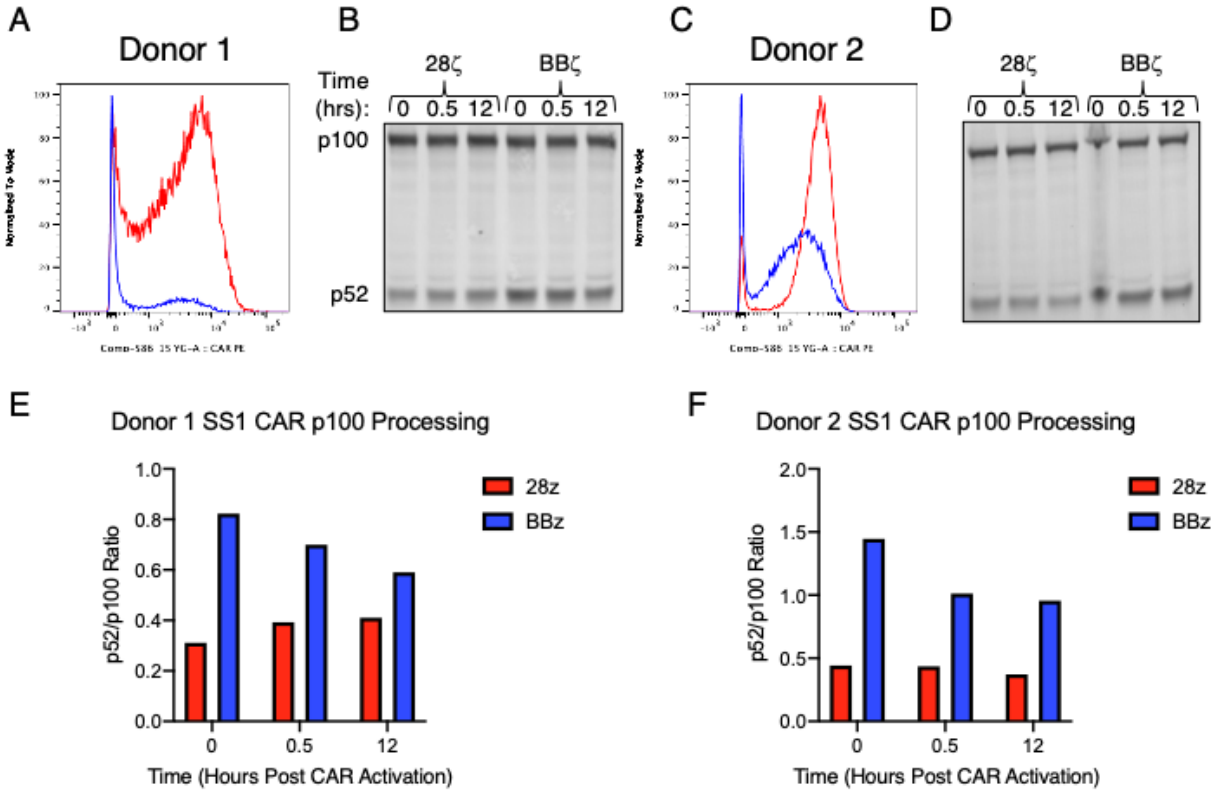

Fig. S7. Anti-mesothelin BBζ CAR also drives ncNF-κB signaling. (**A**) The cell surface expression of 28ζ (red) and BBζ (blue) CARs on live CAR T cells from donor 1 was analyzed by flow cytometry. (**B**) Western blotting analysis of the processing of p100 processing to p52 before and after the addition of mesothelin-coated beads to the indicated CAR T cells from donor 1 at the indicated times. (**C**) The cell surface expression of 28ζ (red) and BBζ (blue) CARs on live CAR T cells from donor 2 was analyzed by flow cytometry. (**D**) Western blotting analysis of the processing of p100 to p52 before and after the addition of mesothelin-coated beads to the indicated CAR T cells from donor 2 at the indicated times. (**E** and **F**) Quantification of the p52/p100 ratio in the indicated CAR T cells from donor 1 (E) and donor 2 (F).

Fig. S8

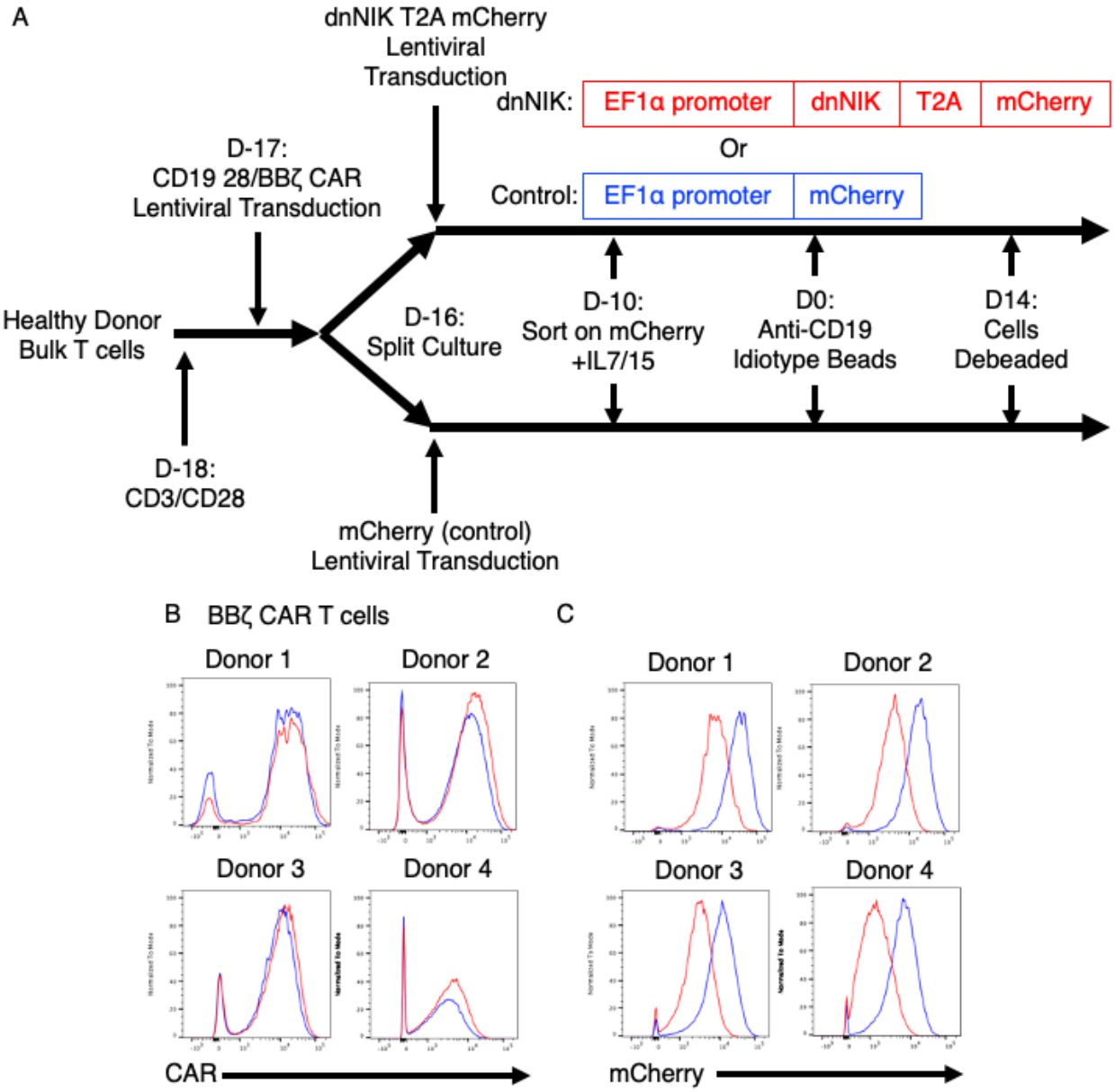

Fig. S8. Dual-transduced T cell production scheme, day 0 CAR, and mCherry expression. (**A**) Dual transduction scheme for the expression of dnNIK in CAR T cells. (**B**) Flow cytometric analysis of the cell surface expression of BBζ CAR on control cells (blue) and dnNIK-expressing (red) CAR T cells from the indicated donors immediately before activation with anti-CD19 idiotype beads. (**C**) Flow cytometric analysis of mCherry in control (blue) and dnNIK-expressing (red) CAR T cells from the indicated donors immediately before activation with anti-CD19 idiotype beads. Data in (B) and (C) are representative of four experiments.

Fig. S9

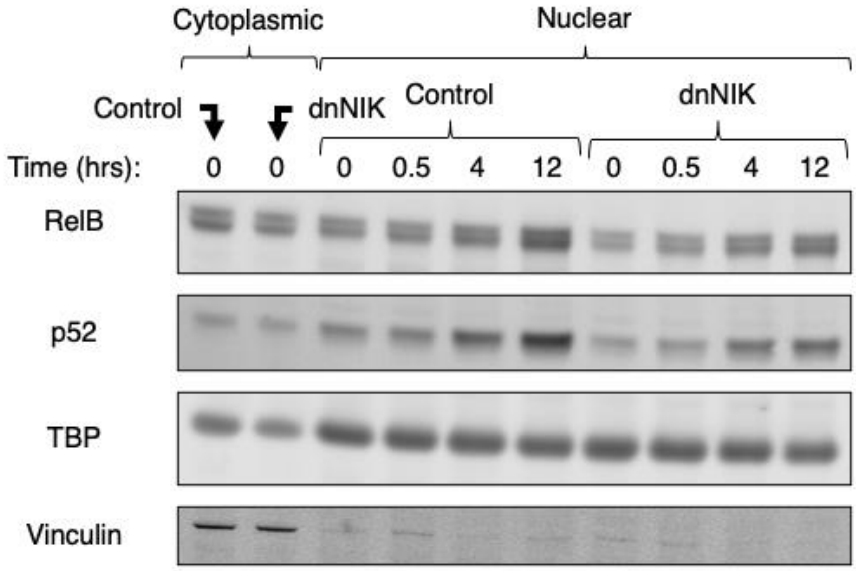

Fig. S9. Western blotting analysis of nuclear and cytoplasmic fractions to compare control and dnNIK-expressing anti-CD19 BBζ T cells. Additional representative Western blotting analysis of the indicated proteins in the cytoplasmic and nuclear fractions of BBζ CAR T cells expressing either mCherry (control) or dnNIK that were incubated for the indicated times with stimulator bead addition. Loss of vinculin indicates the nuclear fractions. These data complement those in Fig. 5, C and D.

Fig. S10

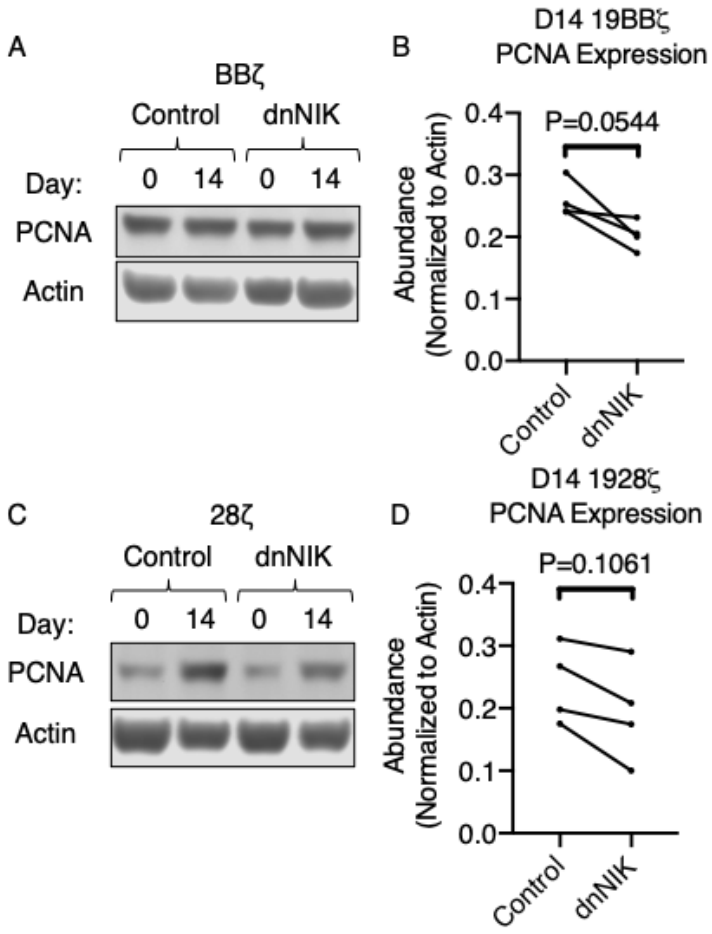

Fig. S10. dnNIK does not affect PCNA abundance in CAR T cells. (**A**) Representative Western blotting analysis of PCNA and actin in BBζ CAR T cells expressing mCherry (control) or dnNIK before or 14 days after the addition of stimulator beads. (**B**) Quantification of the relative abundance of PCNA in the indicated cells from the experiments represented in (A). (**C**) Representative Western blotting analysis of PCNA and actin in 28ζ CAR T cells expressing mCherry (control) or dnNIK before or 14 days after the addition of stimulator beads. (**D**) Quantification of the relative abundance of PCNA in the indicated cells from the experiments represented in (C). *P* values were derived from paired student's *t* test analysis of four donors from four independent experiments.

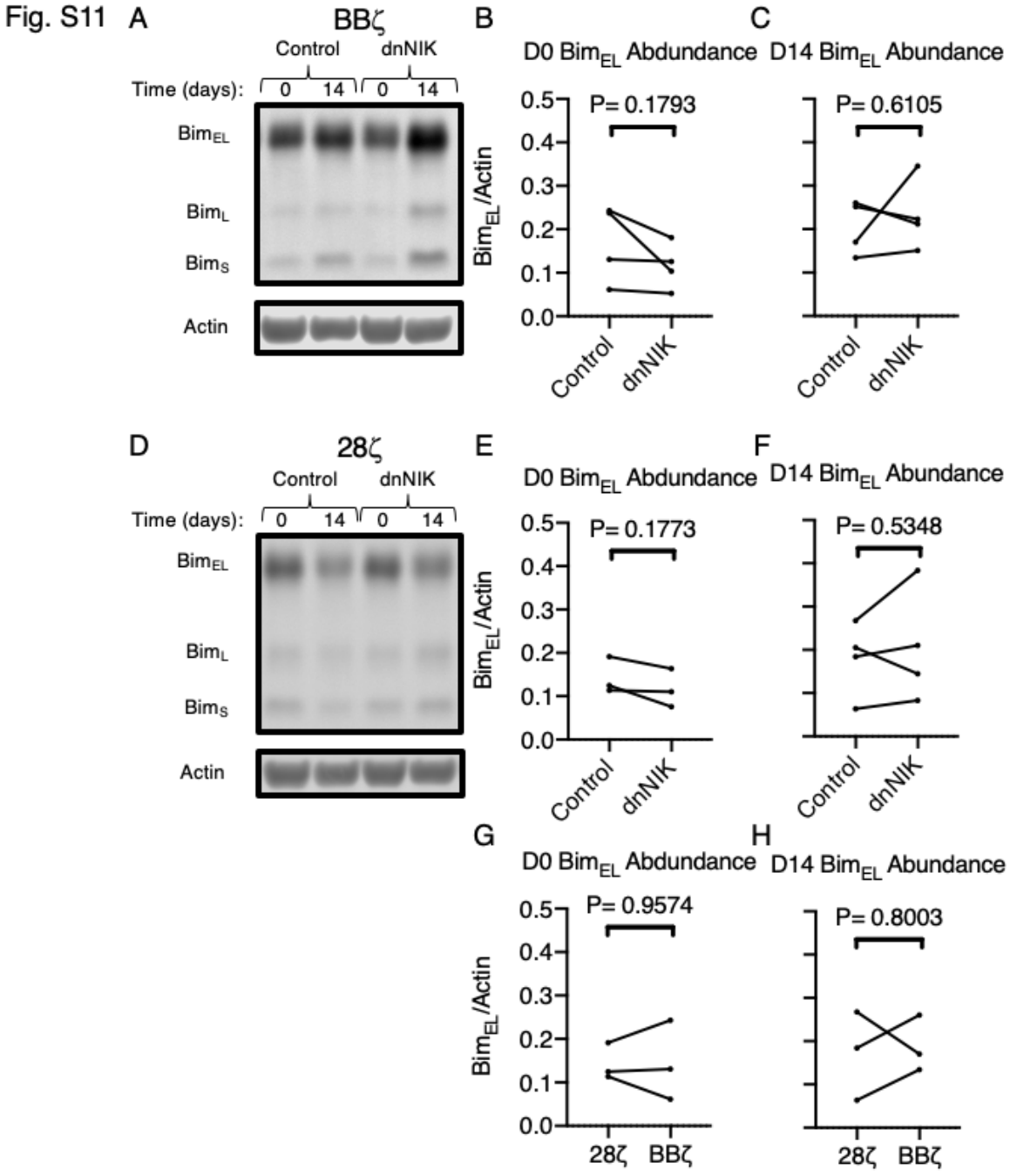

Fig. S11. Bim$_{EL}$ abundance in anti-CD19 CAR T cells. (**A**) Representative Western blotting analysis of the indicated Bim isoforms in control and dnNIK-expressing BBζ CAR T cells (shown in Fig. 6A). (**B** and **C**) Quantification of the relative amounts of Bim$_{EL}$ in the indicated BBζ CAR T cells before (B) and 14 days after (C) the addition of anti-CD19 beads. Data in (B) and (C) are from four donors in four independent experiments. (**D**) Representative Western blotting analysis of the indicated Bim isoforms in control and dnNIK-expressing 28ζ CAR T cells (as shown in Fig. 6F). (**E** and **F**) Quantification of the relative amounts of Bim$_{EL}$ in the indicated 28ζ CAR T cells before (E) and 14 days after (F) the addition of anti-CD19 beads. Data in (E) are from three donors in three independent experiments. No pre-bead sample was taken for the fourth donor shown in (F). Data in (F) are from four donors in four independent experiments. (**G** and **H**) Comparison of the relative abundance of Bim$_{EL}$ in 28ζ and BBζ CAR T cells before (G) and 14 days after (H) the addition of anti-CD19 beads. Data are from three donors in three independent experiments.

Fig. S12

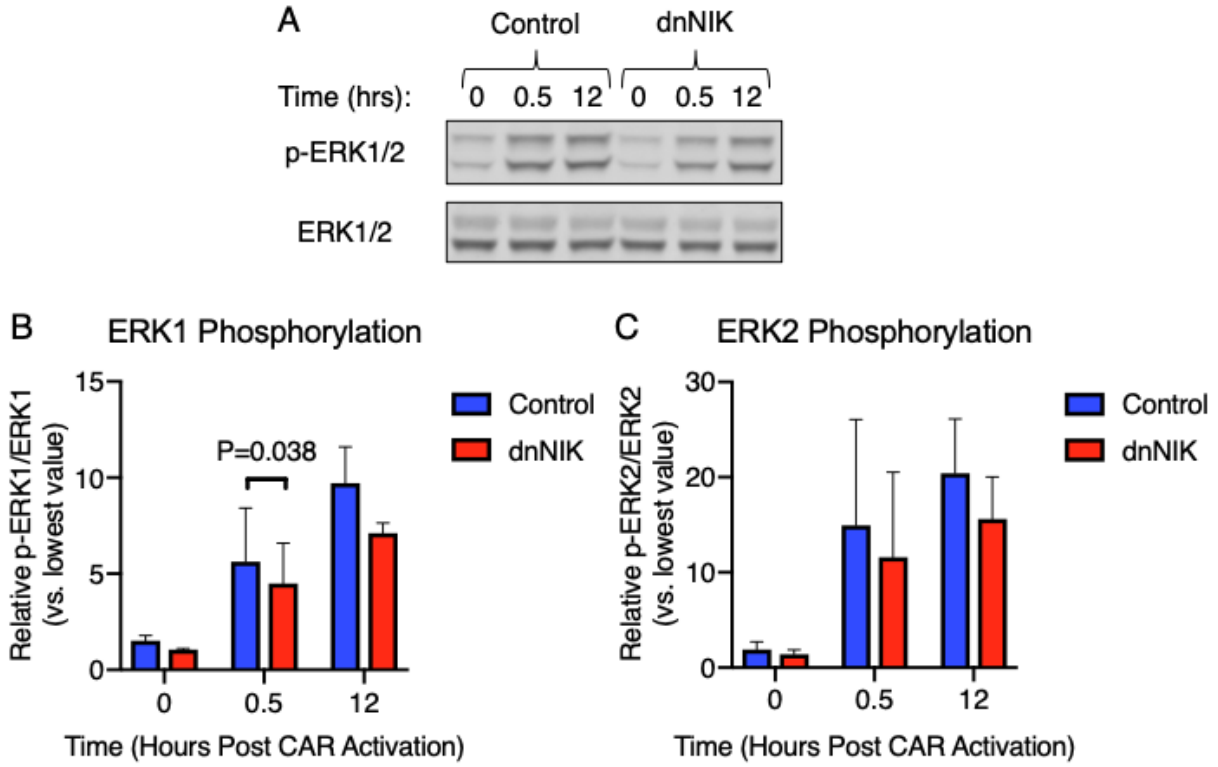

Fig. S12. ERK1/2 phosphorylation in control and dnNIK-expressing BBζ CAR T cells. (**A**) Representative Western blotting analysis of total and phosphorylated ERK1/2 proteins in BBζ CAR T cells expressing mCherry (control) or dnNIK at the indicated times after the addition of stimulator beads. (**B** and **C**) Quantification of the normalized amounts of phosphorylated ERK1 (B) and phosphorylated ERK2 (C) in the indicated cells from the experiments represented in (A). *P* values were derived from two-way ANOVA with Holm-Sidak's multiple comparisons test of three donors from three independent experiments.

Fig. S13

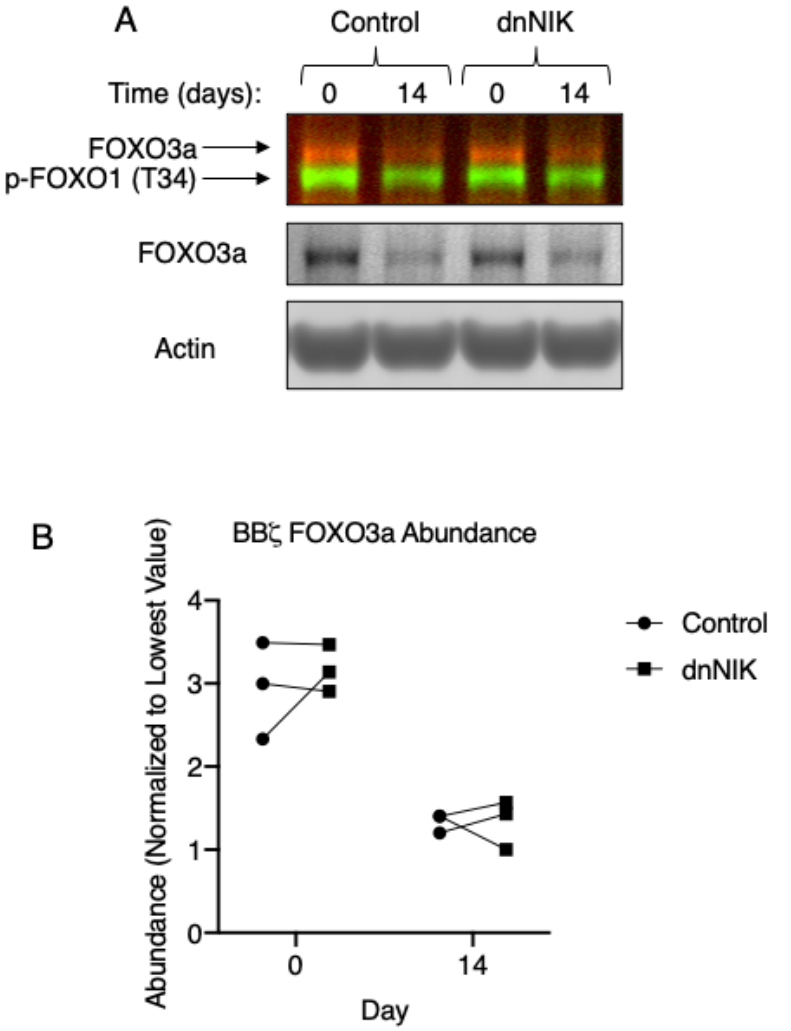

Fig. S13. FOXO3a abundance and phosphorylation in control and dnNIK-expressing BBζ CAR T cells. (**A**) Representative Western blotting analysis of FOXO3a abundance and FOXO1 phosphorylation in anti-CD19 BBζ CAR T cells expressing mCherry (control) or dnNIK at the indicated times after the addition of stimulator beads. (**B**) Quantification of the relative amounts of FOXO3a in the indicated cells at the indicated times from the experiments represented in (A). *P* values were calculated by two-way ANOVA with Tukey's multiple comparisons test of three donors from three independent experiments.

Fig. S14

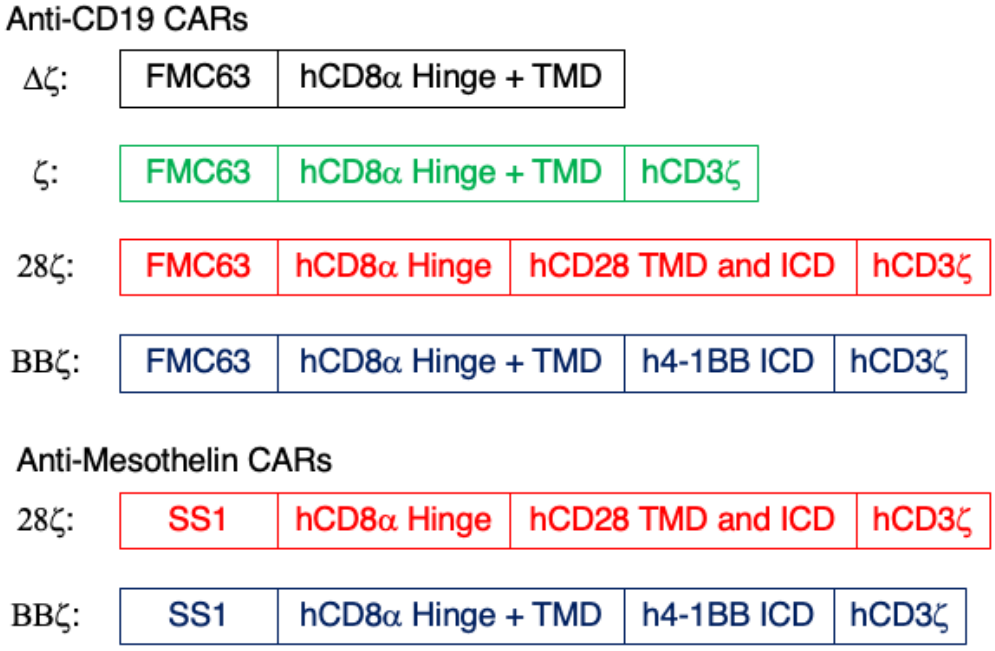

Fig. S14. CAR constructs. The anti-CD19 CARs were previously described by Milone *et al*. (*41*). The anti-mesothelin CARs were previously described by Carpentino e*t al*. (*96*). h, human; TMD, transmembrane domain; ICD, intracellular domain.

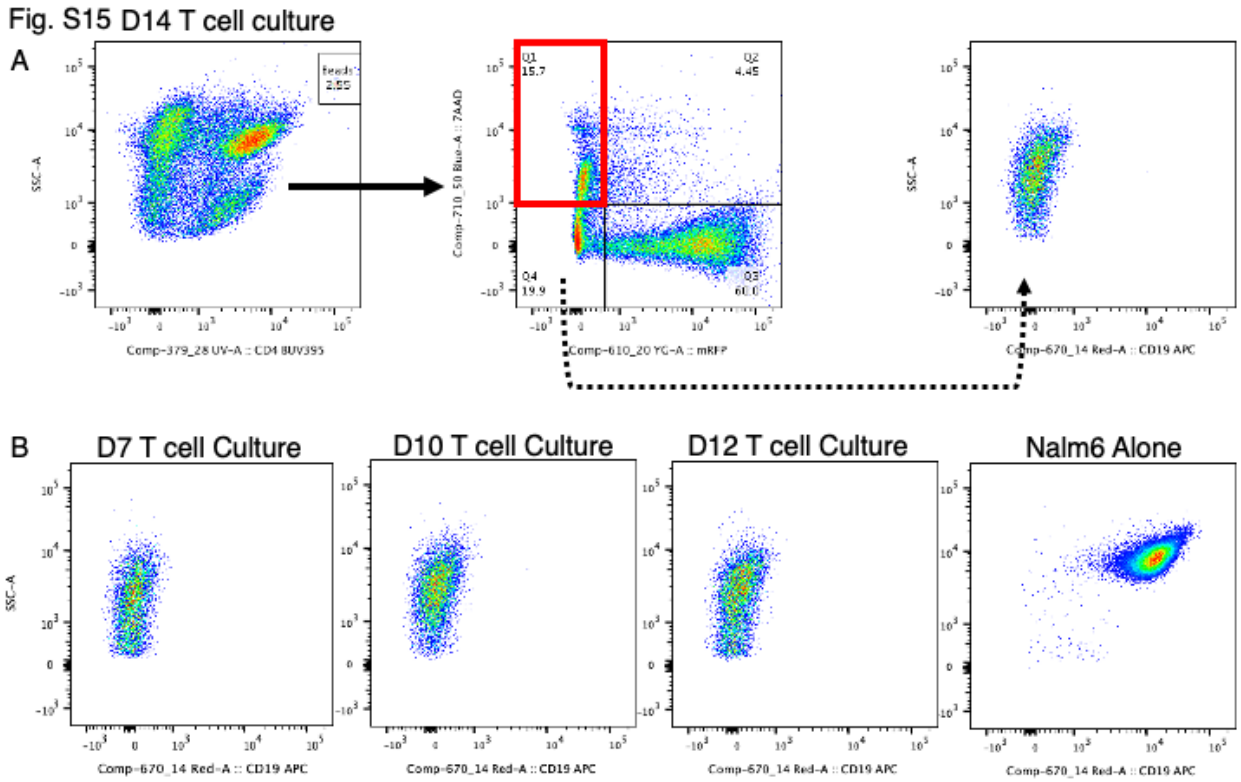

Fig. S15. Representative gating strategy to quantify cell death by flow cytometry and assess the elimination of CD19$^+$ Nalm6 cells. (**A**) Gating strategy for T cell cultures on day 14. 7AAD$^+$mRFP$^-$ events were counted as dead cells. 7AAD$^-$mRFP$^-$ events were assessed for CD19 expression. (**B**) All mCherry-negative, 7AAD-negative cells stained for CD19 before the second round of incubation with irradiated Nalm6 cells (day 7), 3 days later (day 10), and 5 days later (day 12). All mCherry-negative, 7AAD-negative events from parallel cultures of Nalm6 cells alone on day 14 are shown for the CD19$^+$ control.